J Mater Sci (2008) 43:6267–6271
DOI 10.1007/s10853-008-2908-3

Crystal structure and properties of $BaTiO_3$–$(Bi_{0.5}Na_{0.5})TiO_3$ ceramic system

Lanfang Gao · Yanqiu Huang · Liang Liu · Tiantian Liu · Chunfeng Liu · Fei Zhou · Xinwu Wan

Received: 29 January 2008 / Accepted: 28 July 2008 / Published online: 13 August 2008

Abstract $(1 - x)BaTiO_3$–$x(Bi_{0.5}Na_{0.5})TiO_3$ (x ranged from 0.01 to 0.96) ceramics were fabricated by the conventional ceramic technique. The crystal structure, as well as dielectric and piezoelectric properties of the ceramics were studied. All the ceramics formed single-phase solid solutions with perovskite structure after sintering in air at 1150–1250 °C for 2–4 h. The crystal structure and microstructure varied gradually with the increase of $(Bi_{0.5}Na_{0.5})TiO_3$ (BNT) content. The Curie temperature, T_c, shifted monotonously to high temperature as BNT increased. The ceramics with 20–90 mol% BNT had relatively low and stable dielectric loss characteristics. The piezoelectric constant, d_{33}, enhanced with the increase of BNT content through a maximum value in a composition of 93 mol% BNT and then tended to decrease. The maximum value, 148 pC/N, of piezoelectric constant d_{33} together with the electromechanical coupling factors, k_t, 19.8% and k_p, 15.8%, were obtained when BNT was 93 mol%.

Introduction

Piezoelectric ceramics are important materials that are widely used for piezoelectric actuators, sensors, and transducers. The most present widely used piezoelectric ceramics are lead-based materials such as lead zirconate titanate (PZT), which will cause environmental pollution by volatilization of toxic PbO during high-temperature sintering. Therefore, it is necessary to develop lead-free piezoelectric ceramics to replace the lead-based ones.

In recent years, several lead-free piezoelectric ceramic systems such as $BaTiO_3$-based oxides [1–3], $Bi_{0.5}Na_{0.5}TiO_3$-based oxides [4, 5], bismuth layer structure oxides [6–8], and potassium sodium niobate based ceramics [9, 10] have been studied. Among these systems, $(Bi_{0.5}Na_{0.5})TiO_3$–$BaTiO_3$ (abbreviated to BNT–BT) system has been found to be a promising lead-free piezoelectric material, for $(1 - x)Bi_{0.5}Na_{0.5}TiO_3$–$xBaTiO_3$ system has a rhombohedral (F_α)–tetragonal (F_β) morphotropic phase boundary (MPB) at $x = 0.06$–0.07, where the system shows outstanding piezoelectric and dielectric properties [11]. Many researches have been focused on the systems near the MPB composition [11–16]. Only a few reports are involved with the compositions close to $BaTiO_3$ (BT) [17, 18], and there is little information about the BT–BNT solid solution ceramics with the composition from MPB to BT-rich zone. In this work, the $(1 - x)$BT–xBNT systems with different content of BNT were fabricated, and the crystal structure, phase transition, and dielectric and piezoelectric properties of the solid solutions were studied.

Experimental

The $(1 - x)BaTiO_3$–$x(Bi_{0.5}Na_{0.5})TiO_3$ (x ranged from 0.01 to 0.96) (abbreviated as BT–BNT100x) ceramics were prepared by the conventional ceramic technique. The starting raw materials were reagent grade TiO_2, Bi_2O_3, $BaCO_3$, and Na_2CO_3. After mixing in stoichiometric proportions, the

L. Gao · Y. Huang (✉) · L. Liu · T. Liu · C. Liu · F. Zhou · X. Wan
Faculty of Materials Science and Chemical Engineering, China University of Geosciences, Wuhan 430074, People's Republic of China
e-mail: y.q.huang@163.com

Y. Huang
Key Laboratory of Ferroelectric and Piezoelectric Materials and Devices of Hubei Province, Hubei University, Wuhan 430062, People's Republic of China

starting materials were milled in ethanol for 10 h, then dried and calcined at 850 °C for 4 h. The calcined powders were reground, and then pressed into discs with 20-mm diameter and about 1-mm thickness. The green discs were sintered in air atmosphere at 1150–1250 °C for 2–4 h. Silver paste was fired on the surfaces of the discs as electrodes.

The crystal structure of the ceramics was determined by X-ray powder diffraction (XRD). The microstructure of the ceramics was studied by a scanning electron microscope (SEM). Dielectric measurements were carried out by a TH2819 Precision LCR Meter at a frequency of 1 kHz. The electromechanical coupling coefficients (k_p and k_t) were determined using the impedance analyzer according to the resonance method. The piezoelectric constant d_{33} was measured by a ZJ-3A quasi-static piezoelectric d_{33} meter.

Results and discussion

Figure 1 shows the XRD patterns of the $(1 - x)BaTiO_3$–$x(Bi_{0.5}Na_{0.5})TiO_3$ ceramics with 1, 10, 20, 40, 60, 80, 90, 93, and 96 mol% BNT. It indicates that all the ceramics formed single-phase solid solutions with pervoskite structure. The solid solutions are of tetragonal symmetry when BNT content is 1 to 90 mol%. The peaks of (001), (100), (002), and (200) significantly reduce and shift slightly to high degree as BNT content increases. When BNT content is 93 mol%, a broadening peak appears between 46 and 48°, suggesting that tetragonal phase coexists with rhombohedral phase. However, when BNT content is 96 mol%, the solid solutions are of rhombohedral symmetry, which is characterized by a (003)/(021) peak splitting at 2θ between 38 and 42° and a single peak of (202) between 45 and 48° [19]. The peak of (202) is sharp, which implies that no tetragonal phase coexists with rhombohedral phase. This differs from previous results, where rhombohedral and tetragonal phases coexist when BNT content is 92–96 mol% (BT content is 4–8 mol%) [11, 19].

Figure 2 shows the SEM micrographs of the ceramics with different content of BNT. It is found that the shape of the crystal grains changes obviously as BNT increases. The grain size is about 1–2 μm, changing a little with the increase of BNT. All the ceramics have a dense microstructure. In addition, the ceramics with high BNT content have a few micropores. These characteristics indicate a gradual change in crystalline structure and microstructure with BNT concentration.

Figure 3 shows the temperature dependence of the relative permittivity, ε_r, and loss tangent, tan δ, of the ceramics with different BNT content. It is found that the curves of ε_r–T and tan δ–T vary obviously with the content of BNT. The shape of the ε_r–T curves near the Curie point becomes broad as BNT increases, indicating that diffuse phase transition took place. When BNT content is higher than 60 mol%, the three phases of ferroelectric, anti-ferroelectric, and paraelectric, which exist in a wide temperature range,

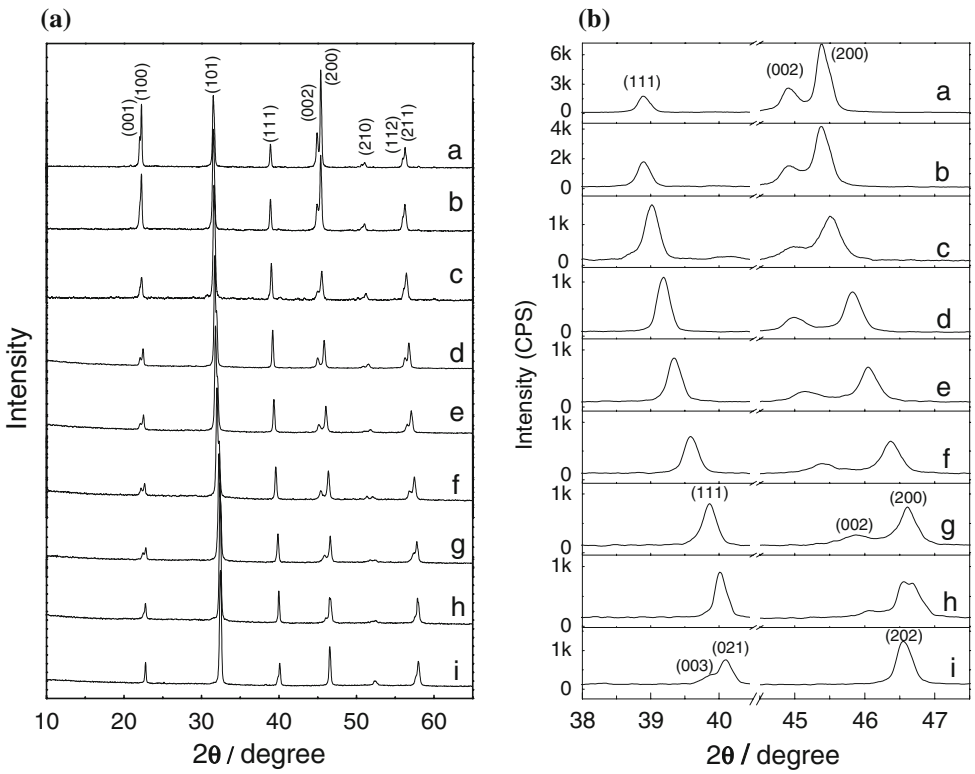

Fig. 1 XRD patterns of BT–BNT100x ceramics of a, BT–BNT1; b, BT–BNT10; c, BT–BNT20; d, BT–BNT40; e, BT–BNT60; f, BT–BNT80; g, BT–BNT90; h, BT–BNT93; i, BT–BNT96. (**a**) Wide range and (**b**) selected portions

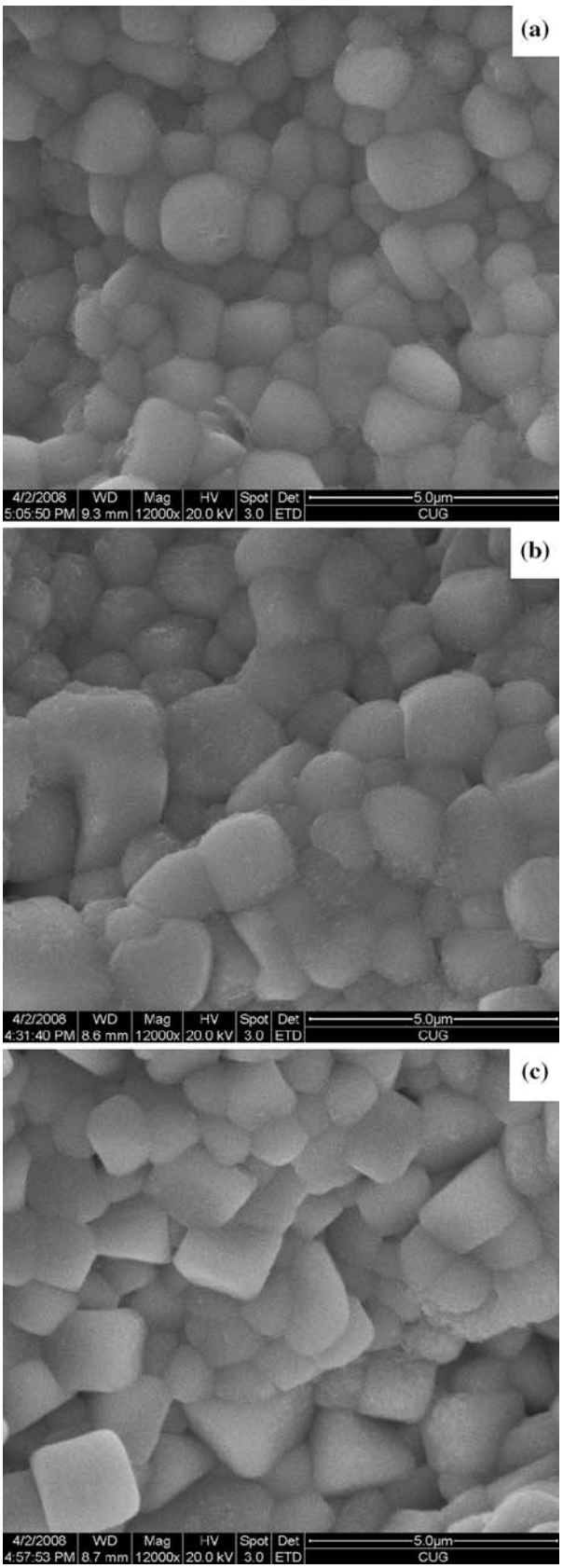

Fig. 2 SEM micrographs for BT–BNT100*x* ceramics. (**a**) BT–BNT30, (**b**) BT–BNT60 and (**c**) BT–BNT90

can be recognized by anomalies of the dielectric constant and loss tangent. These characteristics are similar to the result obtained by Takenaka et al., who researched the BNT–BT system near the MPB composition [11]. The Curie temperature, T_c, shifts monotonously from 118 to 246 °C when BNT content increases from 1 to 90 mol%. These variation characteristics are summarized in Fig. 4.

The permittivity and dielectric loss were affected obviously by BNT content. Figure 5 shows the variation of the permittivity and the dielectric loss at the room temperature with different BNT contents. The permittivity of the ceramics with 1 to 40 mol% BNT decreases from 3000 to about 600, whereas the permittivity of the ceramics with 40–90 mol% BNT increases monotonously from 600 up to 2180. The minimum value of the permittivity at room temperature was obtained when BNT content is 40 mol%. All the ceramics have relatively low dielectric loss, which fluctuates between 0.03 and 0.058 except that of the ceramic with 10 mol% BNT. The curve of tan δ–T of the ceramic with 10 mol% BNT displays a peak at about 32 °C. At the same position, a broad peak appears in the ε_r–T curve. This phenomenon implies that an intermediate phase transition took place at about 32 °C for the sample with 10 mol% BNT. The tan δ of the ceramics with 20–90 mol% BNT almost keep constant through a wide temperature range, indicating that the ceramics have stable dielectric loss characteristics.

Figure 6 shows piezoelectric constant, d_{33}, of the ceramics with different content of BNT. It is found that the d_{33} enhances with the increase of BNT content through a maximum value ($d_{33} = 148$ pC/N) in a composition of 93 mol% BNT and then tends to decrease. This is generally in agreement with previous results, where the maximum value of d_{33} of the BNT–BT ceramics was obtained in a composition near the MPB [12, 14, 15, 19].

Figure 7 shows the electromechanical coupling factors, k_t and k_p, with BNT content. The thickness electromechanical coupling factor, k_t, varies between 15.6 and 26.8%, with a trend to increase with increasing BNT. The planar electromechanical coupling factor, k_p, varies between 13.9 and 18.8%, with a trend similar to k_t as BNT increases. The tendency of dielectric constant $\varepsilon_{33}^T/\varepsilon_0$ and the dissipation factor tan δ of the poled ceramics with the content of BNT are shown in Fig. 8. In a wide range of BNT content, the $\varepsilon_{33}^T/\varepsilon_0$ of ceramics varies between 419 and 613, but increases obviously when BNT content is 93 mol%. All the poled ceramics have relatively low tan δ, which varies between 0.024 and 0.038.

Figure 9 shows the mechanical quality factor Q_m and frequency constant N_p of the ceramics with BNT content. It can be seen that most of the samples have Q_m value in the range of 50–80, except that of the sample with 30 mol% BNT, which has the lowest value of Q_m. When the content

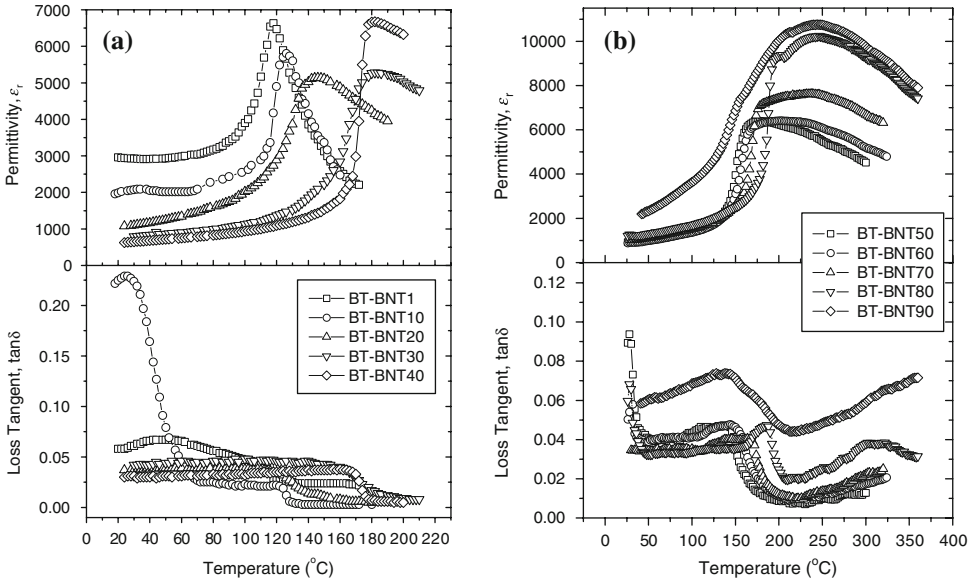

Fig. 3 Temperature dependence of permittivity and loss tangent of the ceramics with different BNT content at 1 kHz. (**a**) The samples with 1–40 mol% BNT. (**b**) The samples with 50–90 mol% BNT

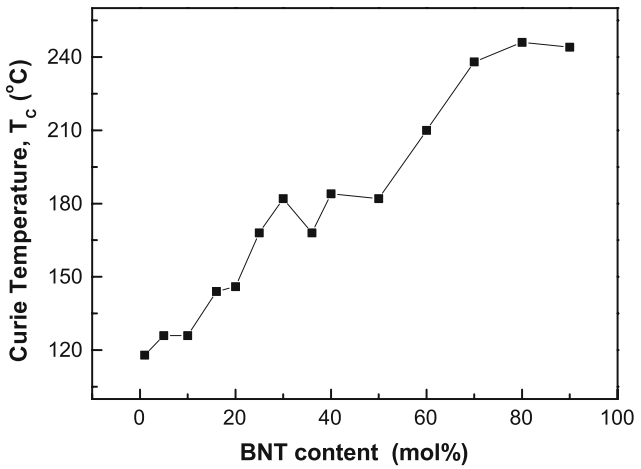

Fig. 4 Curie temperature, T_c, versus the BNT content for the BT–BNT100x ceramics

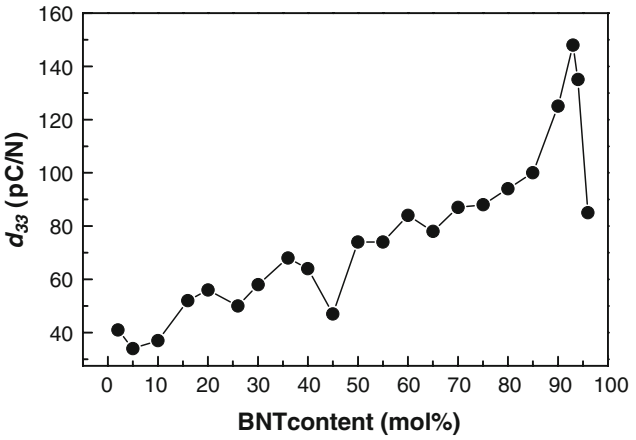

Fig. 6 Piezoelectric constant, d_{33}, versus the BNT content for the BT–BNT100x ceramics

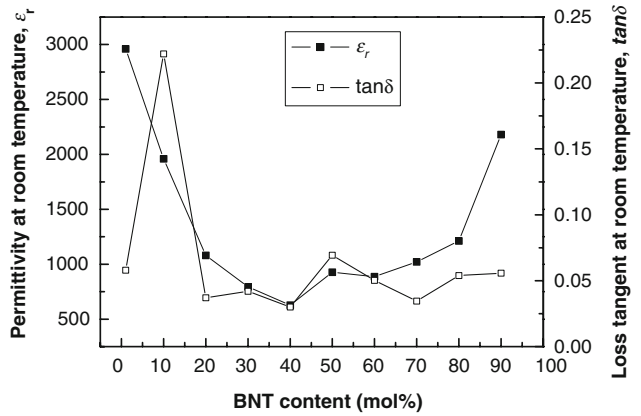

Fig. 5 Permittivity, ε_r, and loss tangent, tan δ, at room temperature versus the BNT content for the BT–BNT100x ceramics at 1 kHz

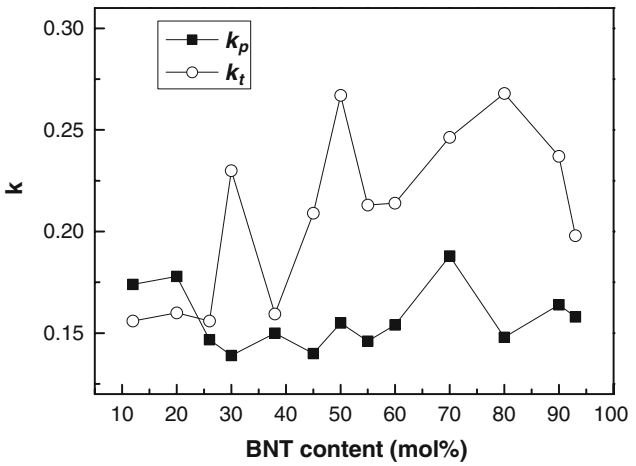

Fig. 7 Electromechanical coupling factors, k_p and k_t, versus the BNT content for the BT–BNT100x ceramics

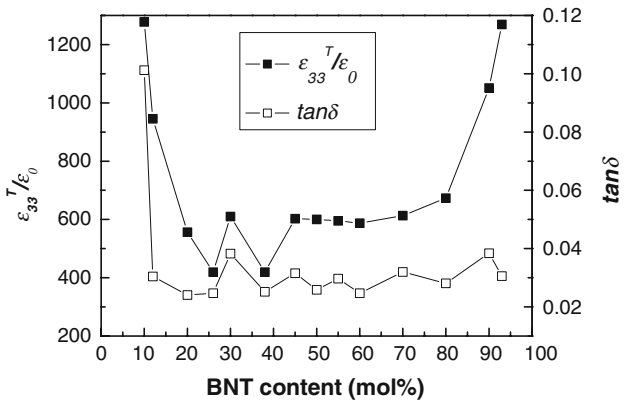

Fig. 8 Dielectric constant $\varepsilon_{33}^{T}/\varepsilon_0$ and the dissipation factor tan δ versus the BNT content for the BT–BNT100x ceramics

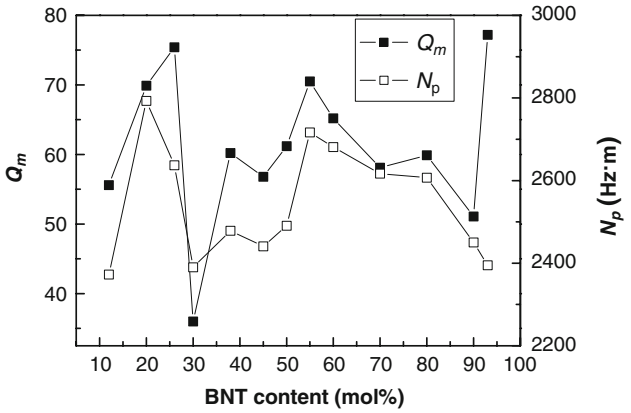

Fig. 9 Mechanical quality factor, Q_m, and frequency constant, N_p, versus the BNT content for the BT–BNT100x ceramics

of BNT is lower than 30 mol%, the Q_m increases as BNT increases. When the content of BNT is higher than 30 mol%, Q_m increases initially and then decreases with the increase when BNT, but increases obviously as BNT content is 93 mol%. The frequency constant N_p shows a similar tendency as the Q_m. The maximum value of N_p is obtained when BNT content is 20 mol%.

Conclusions

The crystal structure, microstructure, and dielectric and piezoelectric properties of the $(1-x)BaTiO_3$–$x(Bi_{0.5}Na_{0.5})TiO_3$ (x ranged from 0.01 up to 0.96) ceramics have been investigated. All the ceramics formed single-phase solid solutions with a pervoskite structure. The crystal structure and microstructure varied with the increase of BNT content. Diffuse phase transition occurred as BNT increased. The Curie temperature, T_c, shifted monotonously from 118 to 246 °C when BNT content increased from 1 to 90 mol%. The ceramics with 20 to 90 mol% BNT had relatively low and stable dielectric loss characteristics. The piezoelectric constant, d_{33}, enhanced with the increase of BNT content through a maximum value in a composition of 93 mol% BNT and then tended to decrease. The maximum value, 148 pC/N, of piezoelectric constant d_{33} together with the electromechanical coupling factors, k_t, 19.8% and k_p, 15.8%, were obtained when BNT was 93 mol%.

Acknowledgements This work was jointly supported by Key Laboratory of Ferroelectric and Piezoelectric Materials and Devices of Hubei Province, Hubei University, China and the Research and Innovation Foundation of graduate student of China University of Geosciences, China (Grant No. CUGYJS0703). The authors are grateful to Professor Suxin Zhang, State Key Laboratory of Geological Processes and Mineral Resources, China University of Geosciences, for SEM observations, and Mr. Jishun Yu for XRD analysis and Ms. Michun Yang for assistance in performing the dielectric and piezoelectric property measurements.

References

1. Ravez J, Simon A (2000) Phys Stat Sol A 178:793. doi:10.1002/1521-396X(200004)178:2<793::AID-PSSA793>3.0.CO;2-X
2. Farhi R, El Marssi M, Simon A, Ravez J (1999) Eur Phys J B 9:599. doi:10.1007/s100510050803
3. Yu Z, Ang C, Guo R (2002) Mater Lett 61:326. doi:10.1016/j.matlet.2006.04.098
4. Peng C, Li JF, Gong W (2005) Mater Lett 59:1576. doi:10.1016/j.matlet.2005.01.026
5. Nagata H, Takenaka T (2001) J Euro Ceram Soc 21:1299. doi:10.1016/S0955-2219(01)00005-X
6. Villegas M, Caballero AC, Moure C, Duran P, Fernandez JF (1999) J Am Ceram Soc 82(9):2411
7. Gelfuso MV, Thomazini D, Eiras JA (1999) J Am Ceram Soc 82:2368
8. Megriche A, Lebrun L, Troccaz M (1999) Sens Actuators A 78:88. doi:10.1016/S0924-4247(99)00223-X
9. Guo Y, Kakimoto K, Ohsato H (2004) Solid State Commun 129:279. doi:10.1016/j.ssc.2003.10.026
10. Chang Y, Yang Z, Chao X (2007) Mater Lett 61:785. doi:10.1016/j.matlet.2006.05.065
11. Takenaka T, Maruyama K, Sakata K (1991) Jpn J Appl Phys 30:2236. doi:10.1143/JJAP.30.2236
12. Takenaka T, Huzumi A, Hata T, Sakata K (1993) Silic Ind 7:136
13. Hosono Y, Harada K, Yamashita Y (2001) Jpn J Appl Phys 40:5722. doi:10.1143/JJAP.40.5722
14. Chu BJ, Chen DR, Li GR, Yin QR (2002) J Eur Ceram Soc 22:2115. doi:10.1016/S0955-2219(02)00027-4
15. Wang XX, Chan HLW, Choy CL (2003) Solid State Commun 125:395. doi:10.1016/S0038-1098(02)00816-5
16. Li HD, Feng CD, Yao WL (2004) Mater Lett 58:1194. doi:10.1016/j.matlet.2003.08.034
17. Gomah-Pettry JR, Saïd S, Marchet P, Mercurio JP (2004) J Eur Ceram Soc 24:1165. doi:10.1016/S0955-2219(03)00473-4
18. Takeda H, Aoto W, Shiosaki T (2005) Appl Phys Lett 87:102104. doi:10.1063/1.2042551
19. Xu Q, Chen S, Chen W (2004) J Alloy Comp 381:221. doi:10.1016/j.jallcom.2004.02.057